Journal of Power Sources 243 (2013) 668–675

Contents lists available at SciVerse ScienceDirect

Journal of Power Sources

journal homepage: www.elsevier.com/locate/jpowsour

Influence of isovalent ions (Ca and Mg) on the properties of $LiCo_{0.9}M_{0.1}PO_4$ powders

Lucangelo Dimesso*, Christina Spanheimer, Wolfram Jaegermann

Technische Universitaet Darmstadt, Materials Science Department, Petersenstrasse 32, D-64287 Darmstadt, Germany

HIGHLIGHTS

- Preparation of $LiCo_{0.9}\boldsymbol{M}_{0.1}PO_4$ ($\boldsymbol{M}$ = Co, Mg, Ca) powders by 2-steps anneal process.
- Investigation of the prepared materials in dependence on Mg and Ca substitution.
- Improvement of the specific capacity (60 mAh g^{-1}) in the $LiCoPO_4$ system.
- Improvement of the specific capacity (68 mAh g^{-1}) in the Ca-substituted system.

ARTICLE INFO

Article history:
Received 27 February 2013
Received in revised form
7 May 2013
Accepted 28 May 2013
Available online 12 June 2013

Keywords:
Sol–gel
Cathode materials
Lithium cobalt phosphate
Isovalent substitution
Calcium
Magnesium

ABSTRACT

$LiCo_{0.9}M_{0.1}PO_4$ (M = Co^{2+}, Mg^{2+}, Ca^{2+}) compounds are synthesized by Pechini-assisted sol–gel process and after annealing at 300 °C for 5 min in air, then at 730 °C for 12 h in nitrogen (2-steps annealing process). The XRD-patterns reveal the presence of $LiCoPO_4$ as major crystalline phase and of CoP_2O_7 (M = Co), of Co_2P (M = Mg), of Co_2P, Li_3PO_4, $(Ca,Co)_3(PO_4)_2$ (M = Ca) as impurities. The morphological investigation shows a homogenous spongy-like structure for M = Co, and a more compact structure with spherical particles separated on the surface in Mg- and Ca-containing systems. In the voltammetric curves, a very good reversibility with mean peak maxima in the cathodic region of 4.4 V for M = Co, 4.5 V for M = Ca and 4.6 V for M = Mg respectively are observed. The discharge specific capacities, at a discharge rate of C/10 and room temperature, were 60 mAh g^{-1} for M = Co, 36 mAh g^{-1} for M = Mg and 68 mAh g^{-1} for M = Ca respectively. The electrochemical impedance spectroscopy data reveal a decrease of the electrical resistance and the improvement of the Li-ion conductivity after the addition of Ca and Mg-ions into the $LiCoPO_4$ system.

1. Introduction

With the increasing demand for electric and hybrid electric vehicles to resolve energy and environmental problems, there is intensive research activity into alternative electrode materials with high specific energy density, high power density and excellent thermal stability for Li-ion batteries (LIBs) [1]. Olivine-structured orthophosphates $LiMPO_4$ (M = Fe, Mn, Ni and Co) have been proposed as promising alternative to the traditional cathode materials, because of their energy storage capacity combined with electrochemical and thermal stability [1–7]. Particularly, $LiFePO_4$ has drawn much attention because of its low cost and non-toxicity. The Fe^{2+}/Fe^{3+} couple operates around 3.45 V with a theoretical capacity of 170 mAh g^{-1} and provides energy density comparable to that of layered $LiCoO_2$ and spinel $LiMn_2O_4$ cathodes. However, the key issue with $LiFePO_4$ is its one-dimensional lithium-ion diffusion and poor electronic conductivity ($\sim 10^{-9}$ S cm^{-1}). Replacing the transition-metal ion Fe^{2+} by Mn^{2+}, Co^{2+}, and Ni^{2+} increases the redox potential significantly from 3.45 V in $LiFePO_4$ to 4.1, 4.8, and 5.1 V, respectively, in $LiMnPO_4$, $LiCoPO_4$, and $LiNiPO_4$ because of the changes in the positions of the various redox couples. Unfortunately these materials suffer from a number of drawbacks, such as complex synthesis procedures, poor electronic conductivity, that must be overcome before they can compete with $LiFePO_4$. $LiMnPO_4$ is of particular interest because of the environmentally benign manganese and the favorable position of the $Mn^{2+/3+}$ redox couple at 4.1 V vs. Li/Li^+, which is compatible with most of the electrolytes. However, it has been shown to offer very low capacity and poor rate capability due to the large lattice distortions induced by Jahn–Teller active Mn^{3+} ions and the much lower electronic conductivity

* Corresponding author. Tel.: +49 (0) 6151 16 69667; fax: +49 (0) 6151 16 6308.
E-mail address: ldimesso@surface.tu-darmstadt.de (L. Dimesso).

0378-7753/$ – see front matter © 2013 Elsevier B.V. All rights reserved.
http://dx.doi.org/10.1016/j.jpowsour.2013.05.196

($\sim 10^{-14}$ S cm^{-1}) of $LiMnPO_4$ compared to $LiFePO_4$ [4]. The flat voltage profile at 4.8 V of $LiCoPO_4$ is attractive to increase the energy density. However, its full theoretical capacity (~ 167 mAh g^{-1}) has not been realized in practical cells so far, and the cycle life of $LiCoPO_4$ is also poor due to the instability of the commonly used $LiPF_6$ in EC:DEC electrolyte at these high operating voltages [5–7]. The redox potential of $LiNiPO_4$ is even higher at 5.1 V, which makes it hard to test with the currently available electrolytes.

Among the $LiMPO_4$ family, $LiCoPO_4$ is the only example of this class of materials that is suitable for 5 V performances [8]. Further, efforts toward improving the non-aqueous electrolyte have made $LiCoPO_4$ an attractive cathode to explore in the high charge voltage regime, up to 5 V. Although the reversibility of Li-ions extraction–insertion from/into $LiCoPO_4$ was demonstrated in a few reports [5,9–11], a severe capacity fading during cycling has limited the use of this material in practical applications.

Recently, the mixed transition-metal systems have attracted considerable interest. Given their similar ionic radii, it might be expected that Fe, Mn, Co and Ni transition metals are mutually soluble and with isovalent ions. In the case of $LiCo_xFe_{1-x}PO_4$, neutron diffraction revealed that the Co^{2+} ions are distributed randomly over Fe^{2+} sites [12]. Similarly, Islam [13] presented support for the solubility of Mn^{2+}, Co^{2+}, and Ni^{2+} on the Fe site in the $LiFePO_4$ system based on lattice energetics of dopant incorporation. Further, Fisher [14 and references therein] performed a systematic survey of the cathode materials $LiMPO_4$ (M = Mn, Fe, Co, and Ni) by using atomistic simulation techniques to provide detailed insights into defect, dopant, and ion migration properties relevant to their electrochemical behavior. After examination of a variety of dopants with charges of +1 to +5 for both Li^+ and M^{2+} substitution, the authors found low favorable energies only for Na^+ substitution on the Li^+ site and isovalent dopants (e.g. Mg^{2+}) on the M^{2+} site. In contrast, supervalent doping (especially Ti^{4+} and Nb^{5+}) appears unfavurable on both Li^+ and M^{2+} sites in all four phases; the charge-compensation mechanism for such doping in $LiMPO_4$ does not alter the M^{2+} valence state and hence is unlikely to contribute to high electronic conductivity. These results are in accord with recent experimental reports of unsuccessful incorporation of significant levels (>3%) of aliovalent dopants to enhance electronic conductivity.

Olivine-structured $LiCoPO_4$ can be easily prepared by soft chemistry routes [15–18]. By using a Pechini-assisted sol–gel process, our group has reported the preparation of $LiCoPO_4$ powders as well as of $LiFePO_4$–carbon foams composites [19,20]. During the work, we have found out that the annealing atmosphere plays an important role on the structural, morphological and electrochemical properties of the products, On the basis of the obtained results, we optimized the conditions of preparation by performing an annealing at low temperature ($T = 300$ °C) in flowing air, followed by the annealing at higher temperature ($T = 730$ °C) in flowing nitrogen with a grind of the powders between them (hereafter this process is labeled as "2-steps annealing" process). In this work, the influence of the substitution of isovalent Mg- and Ca-ions for Co-ions on the structure, morphology and electrochemical properties of the olivine-structured $LiCoPO_4$, prepared by the 2-steps annealing process, is investigated. The investigated composition (**$LiCo_{0.9}M_{0.1}PO_4$**) has the same stoichiometric ratio of the cathode materials (e.g.: **$LiFe_{0.9}Mg_{0.1}PO_4$**) commercialized by the Valence Technology Inc.

2. Experimental

The experimental procedures for the preparation of the samples were similar to those reported earlier [19,20] and slightly modified for the substituted samples. The $LiCo_{0.9}M_{0.1}PO_4$ (M = Co, Mg, Ca) samples were prepared by dissolving in water $Li(CH_3COO)\cdot 2H_2O$ (lithium acetate), $Co(CH_3COO)_2\cdot 4H_2O$ (cobalt(II) acetate), $Ca(CH_3COO)_2$ (calcium acetate) or $Mg(CH_3COO)_2\cdot 4H_2O$ (magnesium acetate) as precursors (molar ratio 1:1) with citric acid (2 × mol [M]). After that phosphoric acid in equimolar ratio with Li and (Co + M) ions was added. The starting solution, with a concentration of the precursors of 0.1 M, was slowly evaporated at 80 °C under air for 3 h. The homogenous gel was heat-treated in air at 300 °C for 5 min, then under nitrogen at 730 °C 12 h respectively. The samples have been labeled according to the substituting elements, $LiCo_{0.9}$***Mg***$_{0.1}PO_4$ (for M = Mg, hereafter labeled *LCMP*), $LiCo_{0.9}$***Ca***$_{0.1}PO_4$ (for M = Ca, hereafter labeled *LCCP*). In order to compare all the systems by the similar starting composition, the (un-) substituted sample "*$LiCoPO_4$*" can be also written as $LiCo_{0.9}$***Co***$_{0.1}PO_4$ and hereafter it will be labeled *LCP*.

The structural analysis, SEM imaging and electrochemical characterization of the samples were similar to those reported previously [19,20]. The samples were directly assembled in an argon-filled dry box with water and oxygen less than 5 ppm. The typical cathode material was fabricated as follows: 85 wt.% active material, 10 wt.% acetylene carbon black and 5 wt.% PTFE (60 wt.% water dispersion, Aldrich) as binder were intimately mixed in a few milliliters of 2-propanol and treated in a ultrasound bath for 20 min at RT. The resulting paste-like material was cut in pellets and dried out at 80 °C for 24 h under vacuum (resulting electrode containing 20–30 mg active compound). In the cell, Li metal was used as anode, SelectiLyte LF30 (1 M Li-FAP in ethylene-carbonate: dimethyl-carbonate 1:1 (wt/wt), Merck KGaA, Germany) as electrolyte [21,22], Celgard®2500 as separator. Aluminum foils were used as current collectors. The electrochemical impedance spectroscopy (EIS) analysis was carried out by applying an ac voltage of 10 mV over the frequency range from 0.1 Hz to 300 kHz (MultEchem™ Potentiostates, Gamry Instruments, Inc.). All electrical measurements were performed at room temperature.

3. Results and discussion

3.1. Structural analysis

The XRD-spectra of the $LiCo_{0.9}M_{0.1}PO_4$ (M = Co, Mg, Ca) powders are shown in Fig. 1A. All samples exhibit $LiCoPO_4$ as major crystalline phase with an ordered olivine structure indexed to the orthorhombic *Pnma* space group. The enlarged patterns, shown in Fig. 1B, reveal a shift in the positions of the (311) and (121) reflections toward higher diffraction angles in the LCMP system. This shift has been previously observed and reported by Muraliganth [23] during the investigation of carbon-coated $LiFe_{1-y}Mg_yPO_4$, $LiMn_{1-y}Mg_yPO_4$ with $y = 0$, 0.25, 0.50, 0.75 and 1.0, and by Kishore [24] during the investigation of $LiCo_{1-x}M_xPO_4$ (M = Mg^{2+}, Mn^{2+} and Ni^{2+}; $0 \le x \le 0.2$) synthesized by solid state reaction. The authors found out that the shift is related to variations in lattice parameters and unit cell volume and can be understood on the basis of the ionic radii of the various M^{2+} cations (in our case Co^{2+}, 0.745 Å, six-fold coordination, high spin; Mg^{2+}, 0.720 Å, six-fold coordination, high spin [25]). Substitution of smaller Mg^{2+} ions for Co^{2+} ions in the LCMP phase lead to a small decrease in '*a*' and '*b*' lattice parameters [24], that indicates that Mg^{2+} ions were successfully introduced into $LiCoPO_4$ matrix structure, slightly decreasing unit cell volume only.

By substituting Ca^{2+} ions for Co^{2+} ions a shift toward lower diffraction angles has been observed (Fig. 1B). This shift can be also explained on the basis of the ionic radii of the Co^{2+} (0.745 Å, six-fold coordination, high spin) and Ca^{2+} (1.00 Å, six-fold coordination, high spin) [25]. Indeed, a similar behavior has been reported during the investigation of the $Li(Fe,Mn)PO_4$ system where the

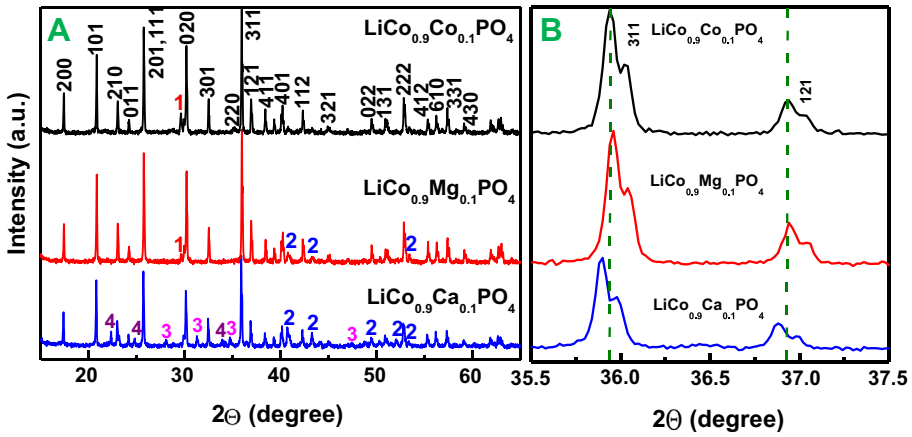

Fig. 1. A) XRD-patterns of the $LiCo_{0.9}M_{0.1}PO_4$ (M = Co, Mg, Ca); B) XRD profiles of the (311) and (121) diffraction peaks only. The secondary phases are indicated as (1) $Co_2P_2O_7$, (2) Co_2P, (3) $(Ca,Co)_3(PO_4)_2$ and (4) Li_3PO_4 respectively.

substitution of the bigger Mn^{2+} ions for the Fe^{2+} caused a shift of the reflections (311) and (121) toward lower diffraction angles [23]. We can reasonably suppose that the substitution of bigger Ca^{2+} ions for Co^{2+} ions in the $LiCoPO_4$ phase lead to an increase of the cell volume and a shift to lower diffraction angles as well.

The XRD diffractograms showed also crystalline peaks which belong to secondary crystalline phases like $Co_2P_2O_7$ (indicated with "1" in Fig. 1A) and particularly Co_2P (indicated with "2" in Fig. 1A) that are usually formed on heating at temperatures higher than 700 °C for longer periods of times ($t \geq 12$ h) in reducing/inert gas atmosphere [19,26]. Furthermore, in the Ca-containing system additional secondary phases like Li_3PO_4 (indicated with "3" in Fig. 1A) and $(Ca,Co)_3(PO_4)_2$ (indicated with "4" in Fig. 1A) with a non-stoichiometric Ca/Co ratio have been observed. The formation of the additional phases could occur due to an excess of the Ca-ions which have not substituted completely the Co-ions into the $LiCoPO_4$ phase. Whether the presence of these secondary phases leads to an improvement of the electrochemical performance of $LiCoPO_4$ is still to be proved.

3.2. Scanning electron microscopy (SEM)

A typical SEM micrograph of the LCP phase after the 2-steps annealing process is shown in Fig. 2A. The morphology consists of a spongy-like structured phase on which very small particles of secondary phase(s). According to our data, the morphology of the powders annealed in 2-steps process is different from that one after annealing in air or in nitrogen only [19]. Indeed, after annealing in air the morphological investigation revealed an interconnected structure through the grain boundaries without secondary phases, whereas after annealing in nitrogen the morphology consisted of aggregates of primary nanoparticles, in shape of prisms, partially embedded in a matrix of amorphous carbon with the presence of secondary phases. As previously stressed up, the annealing conditions play a vital role on the structural, morphological and electrochemical properties of the olivine-structured $LiCoPO_4$ phase. The spongy-like structure, typically detected by using the Pechini (or Pechini-assisted) sol–gel process, is due to the evolution of gaseous by-products during the annealing treatments under the different atmospheres. While the carbon serves as an electron conductor, the pores, when filled with liquid electrolyte, serve as a source of Li^+ ions, that is to say, in this "sponge" approach, the electrolyte layer is formed around a random 3-D network of electrode material. Short transport-path characteristics between the insertion electrodes are preserved with this arrangement.

The addition of the Ca- and Mg-ions affected the morphology of the LCP phase. The SEM micrograph of the LCMP phase (shown in Fig. 2B) revealed the formation of a spongy-like structure and on the surface of this structure, the growth of almost spherical particles can be clearly observed. A similar morphology has been reported by our group [19] during the preparation of the $LiCoPO_4$ phase after annealing at 730 °C for 5 h under nitrogen. The results confirmed the reduction of the Co-containing olivine phosphates leading to the formation of crystallites of metal phosphides (in this case Co_2P). A more complex morphological picture has been

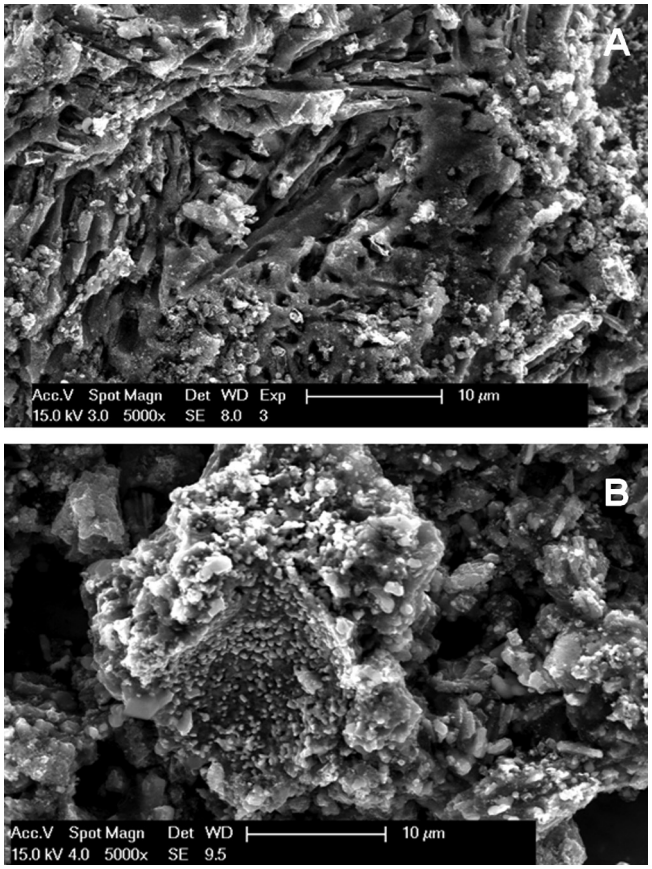

Fig. 2. SEM micrographs of the synthesized A) $LiCo_{0.9}Co_{0.1}PO_4$ and B) $LiCo_{0.9}Mg_{0.1}PO_4$ respectively.

observed in Ca-substituted LCCP systems. The morphological investigation (Fig. S1) revealed the presence of more secondary phases including ribbon-like structures (red arrows in Fig. S1) which could correspond to Co-substituted apatite-like calcium phosphates thermodynamically stable in the temperature range of the annealing under nitrogen [27].

3.3. Electrochemical measurements

Efforts toward improving non-aqueous electrolytes have made $LiCoPO_4$ an attractive cathode to explore in the high charge voltage regime, up to 5 V; however the electrochemical activity of the $LiCoPO_4$ system remains still under controversial debate and has not been fully understood.

Cyclic voltammograms (CVs) for $LiCo_{0.9}M_{0.1}PO_4$ powders using Li metal as counter and reference electrode cycled in the range 3.5–5.3 V are shown in Fig. 3A–C. The deintercalation/intercalation potentials corresponding to the mean peak maxima for the all the samples are shown in Table 1. The CV-curves of the LCP phase show a small shoulder at ~4.92 V in anodic sweep and during reverse sweep a cathodic peak at ~4.40 V (Fig. 3A). The reduction potential of Co^{3+}/Co^{2+} is lower than the value (~4.60–4.65 V) observed by Amine [5], Kishore [24] and by our group [19] after annealing in air or in nitrogen only by reaching a cut-off potential of 5.0 V. This difference may be explained by (i) the higher cut-off potential reached during the anodic sweep in this work (5.3 V) where side reactions cannot be ruled out, (ii) the larger polarization due to the annealing under nitrogen atmosphere as previously reported [19], (iii) a structural re-arrangement in $LiCoPO_4$ that takes place during the charge process of the $LiCoPO_4$ powders. This re-arrangement could be an intrinsic property of the LCP phase and independent of the preparation method as confirmed by similar voltammetric curves reported by Kishore [24] who prepared the LCP phase by a solid state reaction. The asymmetry between the cathodic and anodic CV plots could imply that the Li-ion diffusion in $LiCoPO_4$ powders obeys a different mechanism between charge and discharge processes as proved out recently by Xie [28] by measuring the Li-ion chemical diffusion coefficients on thin films prepared by rf-magnetron sputtering.

Extensive investigations on the electrochemical properties of the Li_xCoPO_4 system prepared by the sol–gel process report the presence of two plateaus in the charge curve (corresponding to $0.7 \leq x \leq 1.0$ and $0 \leq x \leq 0.7$ respectively in the stoichiometric compound) independently of the electrolyte used during the measurements [29,30]. The results support the idea that two-step delithiation is an intrinsic property of the system as also confirmed by using in situ and ex situ XRD to explain the Li extraction/insertion mechanism in $LiCoPO_4$. However, the XRD results showed that the "delithiated" crystalline phase was only a lithium-poor phase; no "$CoPO_4$" was identified even though $LiCoPO_4$ was fully charged [30].

The effects of the Mg-ions and Ca-ions on the CVs of the LCP phase are shown in Fig. 3B and C respectively. The CV-curves of the LCMP phase (Fig. 3B) show a decrease of the voltammetric surface as a function of the anodic and cathodic sweeps and a shift toward higher values of the reduction mean maxima (from 4.52 till 4.63 V). Similar behaviors have been observed in the $Fe^{2+/3+}$ and $Mn^{2+/3+}$ couples with the substitution of Mg^{2+} for Mn^{2+} or Fe^{2+} [23]. The authors argued that the decrease of cathodic and anodic surface in the CV curve is possibly related to the amount of lithium that can be extracted. Indeed, the non transition-metal ions Mg^{2+} do not show any redox behavior and tends to form solid solutions with the transitions metals ions with redox behavior [14 and references therein, 24]. On the other hand, the substitution of redox inactive Mg^{2+} appears to stabilize the redox active $Fe^{2+/3+}$ and

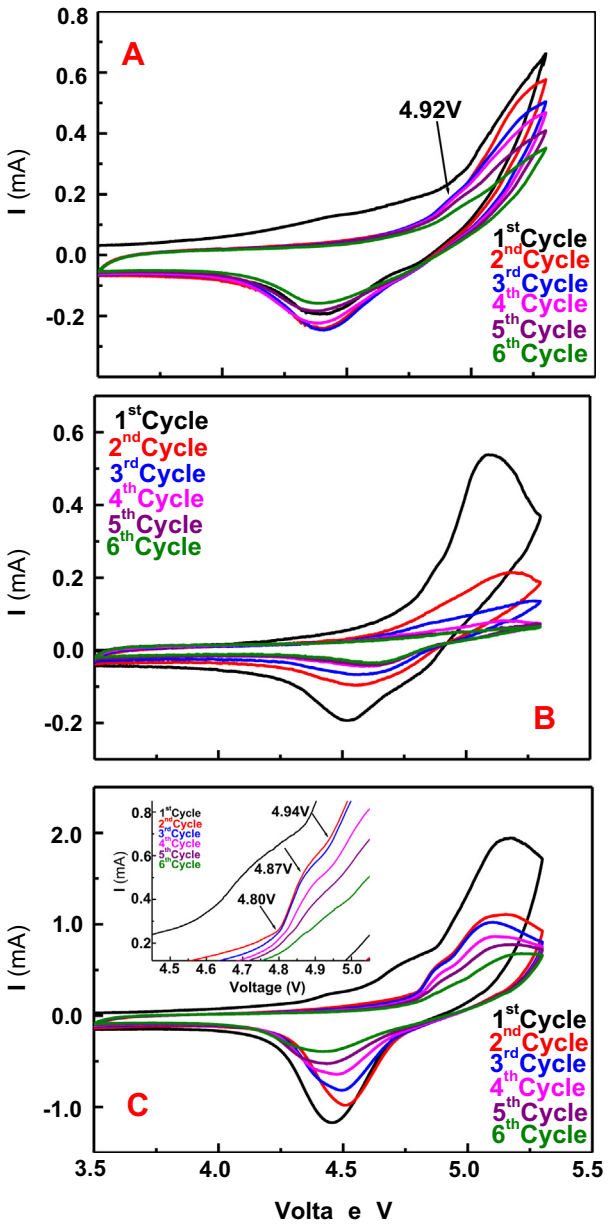

Fig. 3. Cyclic voltammograms recorded for the $LiCo_{0.9}M_{0.1}PO_4$ samples, A) M = Co, B) M = Mg and C) M = Ca respectively (scan rate 0.05 mV s^{-1}, in the potential range 2.5–5.3 V vs. Li^+/Li).

$Mn^{2+/3+}$ couples through the M^{2+}–O–Mg^{2+} interactions leading to a shift of the reduction mean peaks to higher values of potentials.

From the CVs profiles of the LCCP system (Fig. 3C) and the data in Table 1 some important points are noted. Firstly, a decrease of the voltammetric surface as a function of the anodic and cathodic sweeps and a slight shift toward lower values of the reduction mean maxima (from 4.51 till 4.41 V) can be observed. These values are slightly higher than the values of the LCP phase (Table 2) and can be similarly explained by the stabilization of the $Co^{2+/3+}$ couple through the Co^{2+}–O–Ca^{2+} interactions which are weaker compared to the Mg-ions because of the bigger ionic radius. Indeed Fisher [14], during a systematic survey of the cathode materials $LiMPO_4$ (M = Mn, Fe, Co, and Ni) performed by atomistic simulation techniques, argued that the most favorable dopant for M^{2+} is calcium. However, calcium has rarely been investigated as the transfer ion because of its large ionic radius [25], although the standard

Table 1
Values of the deintercalation/intercalation potentials (mean peak maxima in Fig. 3A–C) for the $LiCo_{0.9}M_{0.1}PO_4$ powders.

M	Cycle (nr)	Deintercalation potential (V)	Intercalation potential (V)
Co	1	–	4.41
	2–3	–	4.40
	4	–	4.39
	5–6	–	4.38
Mg	1	5.10	4.52
	2	5.17	4.56
	3	–	4.57
	4	–	4.60
	5–6	–	4.63
Ca	1	5.17	4.46
	2	5.15	4.51
	3–4	5.10	4.49
	5	5.15	4.44
	6	5.18	4.41

electrode potential (−2.87 V vs. SHE) is comparable to that of lithium making it very attractive in terms of the fabrication of high-voltage/energy density batteries [31]. Investigations on biological systems have proved out that Ca-ions are electrochemically active and involved in the most important reactions of living organisms including human mitochondrial cells. Secondly, a shoulder at 4.87 V in the anodic sweeps has been detected and may be related to important electrochemical events. During the anodic sweep, the first change in the CV profile takes place at ∼4.80 V where an increase of the current can be observed; the maximum mean peak of the event occurs at 4.87 V and finally a further change in the CV profile has been detected at 4.94 V. According to the data in the literature [6,28], the events at 4.80 V and 4.94 V correspond to the formation the delithiated phases in agreement with the 2-steps delithiation mechanism formulated by Bramnik [6]. The novelty of our data lies in the shoulder at 4.87 V which is bigger than that observed in the LCP phase (Fig. 3A). This could indicate that the addition of the Ca-ions would favor a greater stabilization of the amorphous delithiated phase and consequently the formation of higher amount of the delithiated phase at disposal for the Li-ions to re-enter into the $LiCoPO_4$ olivine-structured phase. The reversibility of this process is confirmed by the CV-profiles shown in Fig. 3C. These events can lead to an improvement of the electrochemical performance of the LCCP phase compared to LCP one.

The specific capacity as a function of the cycles and the charge and discharge curves (voltage range between 3.5 and 5.3 V) for the first cycle for the LCP, LCCP and LCMP powders after the 2-steps annealing process are shown in Fig. 4A and B respectively. From the data several important points are noted. Firstly, the specific capacity of the LCP phase at the first cycle (60 mAh g^{-1}) increases compared to the values previously reported after annealing in nitrogen (only) and in air (only) [19]. Secondly, the specific capacity of the first charge cycle at high voltage (5.3 V) is lower than the values

Table 2
Content of the residual amorphous carbon (wt.%) of $LiMPO_4$ powders annealed under different conditions (the measured values are an average of repeat determination).

M	Air		Nitrogen		C (wt.%)
	T (°C)	t (min)	T (°C)	t (h)	
Co	300	10	730	12	12.2
Ca	300	10	730	12	10.2
Mg	300	10	730	12	13.4
$LiCoPO_4$	300	30	730	12	5.5[a]

[a] Ref. [20].

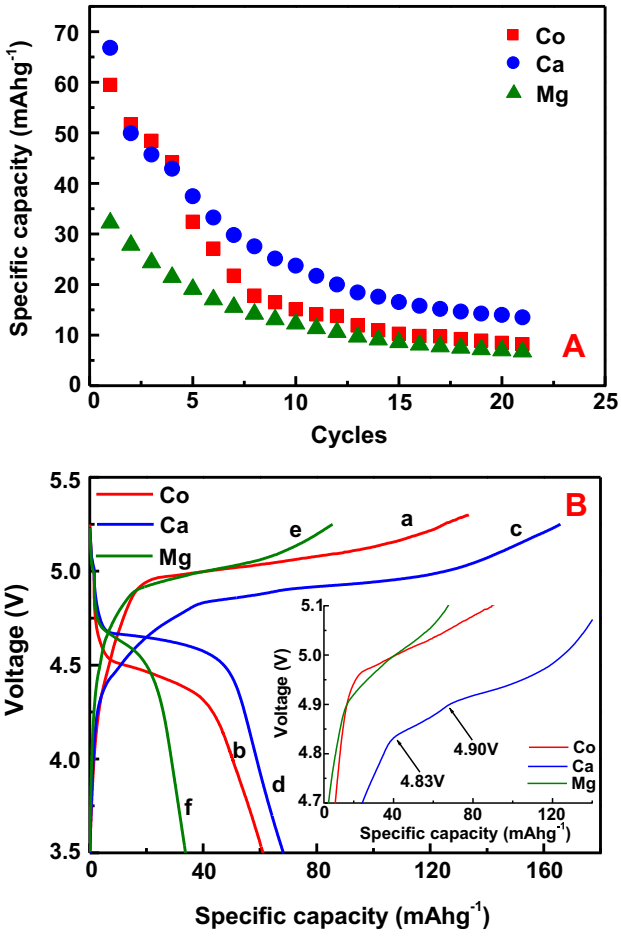

Fig. 4. (A) Discharge capacity measured at a discharge rate of C/10 and room temperature, (B) voltage–capacity curves for the first charge and discharge process, measured at C/10 discharge rate and room temperature for (a, b) $LiCo_{0.9}Co_{0.1}PO_4$, (c, d) $LiCo_{0.9}Ca_{0.1}PO_4$ and $LiCo_{0.9}Mg_{0.1}PO_4$ powders respectively. In the inset, magnification of the first charge curves in the potential range of 4.45–5.05 V.

reported in literature (over 200 mAh g^{-1}) and even lower than the theoretical capacity of the $LiCoPO_4$ system (167 mAh g^{-1}) (curves a, c, e for LCP, LCCP and LCMP systems respectively, in Fig. 4B). Although the decomposition of the electrolyte above 5.0 V, which may lead to an irreversible charge/discharge process, cannot be ruled out this behavior can be better explained by the effect of the carbon and consequently of Co_2P. The content of the carbon has been determined by the elemental analysis (CHN-X) and the results of the investigation are summarized in Table 2. The carbon content in the LCP phase annealed in air for 10 min is higher than the C-content after 30 min [20] confirming further the influence of the annealing conditions. Thirdly, the addition of Ca-ions increases the specific capacity of the first discharge cycle to 68 mAh g^{-1} and decreases the capacity fade whereas the addition of Mg-ions decreases the specific capacity of the first discharge cycle dramatically down to 36 mAh g^{-1}.

The obtained results confirmed strongly the influence of the annealing atmosphere on the electrochemical properties of the olivine-structured $LiCoPO_4$. The annealing atmosphere is strictly related to the formation, the growth and amount of secondary phases such as the residual carbon from the sol–gel process and the formation of Co_2P. Wolfenstine [32] reported that some part of the carbon has been consumed in reducing the $LiCoPO_4$ surface layers to Co_2P, whereas the increase in the amount of metal phosphide with increasing the carbon content is in good agreement with

results of Huang [33] on $LiFePO_4$ who have shown that as the amount of carbon increased the amount of the Fe_2P increased. By plotting the discharge capacity as a function of the added Co_2P, the authors observed the increase of the capacity (to 120 mAh g^{-1}) with increasing the content of Co_2P to ~4–5 wt.%, after that the capacity decreases rapidly with increasing the Co_2P content. The increase in discharge capacity was explained as result of the increase in the electronic conductivity associated with the conductive Co_2P on particles surfaces and with the smaller particle size that results when carbon is present. At higher Co_2P volume fractions the presence of the electrochemically inert Co_2P phase is to decrease capacity by (i) reducing the amount of active $LiCoPO_4$ present and (ii) preventing Li-ions from entering/leaving $LiCoPO_4$ due to its behavior as resistor [19,32]. According to the data reported in Ref. [32], in our case the 2-steps annealing process may reduce the amount of the Co_2P phase and consequently improve the electrochemical performance of the LCCP system.

The addition of Mg- and Ca-ions affects the C-content and the electrochemical properties of the olivine-structured $LiCoPO_4$ cathode material in different ways. The addition of the Mg-ions increased the carbon content into the cathode material to 13.4 wt.% (Table 2) and to a dramatic decrease of the specific capacity (Fig. 4f-curve f) to 36 mAh g^{-1}. The decrease of the specific capacity in solid solutions, in which the non transition-metal ions Mg^{2+} without any redox behavior are substituted for the transition-metal ions with redox behavior, has been already reported for the $LiCoPO_4$ [24] phase and observed in the $LiFePO_4$ and $LiMnPO_4$ olivine-structured materials [23]. The authors explained the decrease of the specific capacity in the LCMP system by the lower number of Li-ions that can be cycled ($1-y$ in the $LiCo_{1-y}Mg_yPO_4$ system, with $y = 0.1$ in our case) [23]. However, the higher carbon content which leads to the formation of higher amount of the ionic "inert" Co_2P phase and the possibly formation of $LiMgPO_4$ in a non-crystalline form could play a role. In the crystalline form, $LiMgPO_4$ and the stoichiometric analogs $LiMnPO_4$ and $LiFePO_4$ are iso-structural with each other and possess octahedral co-ordinations for both the monovalent and divalent cations [34]. However the high stability of $LiMgPO_4$ phase and the electrochemical inertness of the Mg^{2+} ions do not give any contribution to the (de)lithiation processes. Indeed the number of the Li-ions available decreases dramatically by increasing the number of the charge/discharge cycles with a consequent worsening of the electrochemical performance.

The addition of Ca-ions decreases the carbon content down to 10.2 wt.% and increases the specific capacity of circa 10% (68 mAh g^{-1}) compared to the LCP phase. To our best knowledge, the electrochemical properties of solid solutions, in which the non transition-metal ions Ca^{2+} are substituted for the transition-metal ions with redox behavior, have not been reported before. The increase of the specific capacity in the LCCP phase cannot be sufficiently explained by the decrease of the carbon content and consequently by the lower amount of the Co_2P phase. Being the Ca-ions electrochemically active [31,35], this activity is to be taken into account. In addition the high chemical affinity between Ca-ions and phosphate anions could play an important role as well. Indeed Ca^{2+} ions are known as "network modifiers" in the glass science. In a non-crystalline oxide material (or "glass"), constituents can be either *network formers* or *intermediates* or *network modifiers*. The *network formers* (Si, B, Ge) form a highly cross-linked network of chemical bonds. The *intermediates* (Ti, Al, Zr, Be, Mg, Zn) can act as both network formers and modifiers, according to the glass composition. The *network modifiers* (Ca, Pb, Li, Na, K, P_2O_5) alter the network structure; they are usually present as ions, compensated by nearby non-bridging oxygen (NBO) atoms, bound by one covalent bond to the glass network and holding one negative charge to compensate for the positive ion nearby. In our case, the positive influence of the Ca-ions on the electrochemical properties of the LCP phase is revealed by the curve of the first charge cycle (Fig. 4B inset). During the charge process some changes in the slope of the curve can be clearly observed: a first change occurs at a potential of 4.83 V and a second at 4.90 V. The voltage–capacity curve of the LCCP phase for the first charge process is very similar to those we have previously reported which confirmed the coexistence of a "lithiated" and (partially or totally) "delithiated" phases. Interestingly to note is that (i) the change of the slopes take place at voltage values close to those reported in the voltammetric curves (Fig. 3C inset); (ii) the change at 4.90 V corresponds to a value of the specific capacity of 67.6 mAh g^{-1}. This could indicate that during the charge/discharge processes all the Li-ions available participate to the electrochemical performance, that is to say, at potential values higher than 4.90 V the LCCP phase is (totally) delithiated. We can reasonably assume that our measurements give a "snapshot" of delithiated phase making it "visible". Indeed, the Ca-ions seem to favor the stabilization of the "$CoPO_4$ amorphous phase", possibly either due to a re-arrangement of the charge distribution of the non-bridge oxygen atoms ($O\cdots Ca^{2+}\cdots O$) which would stabilize the "$CoPO_4$" phase by avoiding its decomposition through the proposed decomposition reaction:

$$2CoPO_4 \rightarrow Co_2P_2O_7\,(s) + 1/2O_2\,(g) \quad (1)$$

simply avoiding the release of the oxygen during the discharge [36], and/or by the formation of "$LiCaPO_4$" phase in non-crystalline form. In the crystalline form, the structure of $LiCaPO_4$ is composed of a three-dimensional framework of vertex-sharing LiO_4 and PO_4 tetrahedra, which enclose large five-sided channels parallel to the [001] direction, in which the Ca^{2+} ions reside. The Ca^{2+} ions have six short contacts to oxygen and two longer contacts completing an irregular eight-co-ordinate geometry [37] whereas the stoichiometric analogs $LiMnPO_4$, $LiMgPO_4$ and $LiFePO_4$ are iso-structural with each other and possess octahedral co-ordinations for both the monovalent and divalent cations. The formation of the $LiCaPO_4$ phase, even as "intermediate phase", can contribute to the improvement of the (de)lithiation processes of the LCCP phase by favoring the movement of the Li-ions. This fact is supported by studies on the AC conductivity and dielectric behavior of the $LiCaPO_4$ compound as a function of temperature and frequency ranges (200 Hz–5 MHz and 634–755 K respectively) performed by Louati [38]. The impedance and dielectric data confirmed the grain and grain boundary contribution to electrical response in the material. The authors concluded that he electrical conduction in lithium orthophosphate $LiCaPO_4$ compound is presumably caused by the hopping of Li-ions between sites along the [001] direction. Finally, a change of the slope takes place at ~4.95 V and it can be related to side and/or unwanted reactions of the different interface layers among cathode material, electrolyte and anode material [19]. From CV measurements Ni [39] suggested that the highly active Co^{3+} species can catalyze electrolyte decomposition, which accounts for the capacity loss of $LiCoPO_4$ over cycles. Under such circumstance, the charge current passing the electrode does not extract Li ions but oxidize the solvents, leading to decreased real charge capacity than the rated one. In addition, side products may deposit onto the surface of $LiCoPO_4$ electrodes, which attributes to an increased resistance and polarization. As solution, the authors concluded that pre-loading a carbon layer on the surface of $LiCoPO_4$ electrode, the Co^{3+} species was stabilized, and the cyclability was therefore enhanced. In our case, by the addition of the Ca-ions the change of the slope occurs at a very similar potential value (~4.94–4.95 V) observed in the CV-curves and that it is smoother than those reported for the LCP and LCMP phases (Fig. 4B inset) and those after annealing in air or in nitrogen only. If this effect also

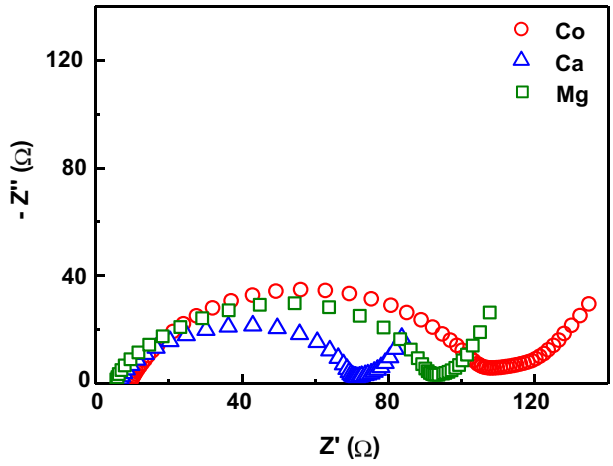

Fig. 5. Nyquist plots of the $LiCo_{0.9}\boldsymbol{M}_{0.1}PO_4$ samples before cycling.

depends upon a greater (electro)-chemical stability of the delithiated phase under the influence of the Ca-ions is still to be cleared.

Despite the improvements obtained by the addition of Ca-ions into the LCP phase, one major challenge for $LiCoPO_4$ cathode, the instability in cycling, remains still unsolved. The instability probably results from various factors such as poor conductivity, solvent oxidation at high voltage, oxygen release, or amorphization induced by fluoridric acid (HF). Nevertheless, our results can open very interesting perspective in the basic research and for technological appliances.

3.4. EIS characterization

Fig. 5 depicts the Nyquist plots of $LiCo_{0.9}M_{0.1}PO_4$ cathode materials for M = Co (open circuit voltage (OCV) of ~2.12 V), M = Ca (OCV of ~2.52 V) and M = Mg (OCV of ~3.16 V) respectively before the cycling. The Nyquist plot of the LCP phase consists of a semicircle alike in appearance of a half ellipse (in the high and intermediate frequency ranges) and a straight line with changing slope to the real axes (in the lower frequency range). Alike, the Nyquist plot of the LCCP and LCMP phases consists of out-of-shaped semicircles (in the high and intermediate frequency ranges) and a straight line inclined with constant slope to the real axes. The study of the ac-impedance results has been performed by using the approach outlined in Ref. [40 and references therein] and Ref. [41].

The R_s, R_1 and CPE_1 values of the prepared cathode materials derived from the equivalent circuit fitting as reported in Ref. [40] are presented in Table 3. Here R_s is the resistance associated with the impedance of the electrolyte (and separator) and consistent with the high frequency intercept in the ac-impedance spectra; R_1 is a component of the ac-impedance semicircle in the high-to-medium frequency range related to the charge transfer resistance and constant phase element CPE_1. As shown by the CV-curves and charge/discharge measurements multiple reactions, which overlap and affect the Li-ions diffusion, occur during the charge/discharge processes in the LCCP and LCMP phases. In order to avoid misunderstandings and misleading conclusions the Warburg element was not included in the fitting of the ac-impedance data.

Table 3
Impedance parameters derived from the equivalent circuit for the $LiCo_{0.9}M_{0.1}PO_4$ systems.

M	R_s (Ω)	R_1 (Ω)	CPE_1-T ($\times10^{-6}$) (F)	CPE_1-P ($\times10^{-6}$)
Co	9.13	104.00	8.75	0.766
Ca	7.91	62.27	0.80	0.174
Mg	6.92	81.06	0.59	0.186

The constant phase element involves two parameters, CPE_1-T which represents the capacity of the whole measured system (anode + cathode) and CPE_1-P which represents a deviation from the capacity [41]. From Fig. 5 and the data reported in Table 3 some important observations can be drawn. The decrease of Rs and of R_1 values by the addiction of the Ca^{2+}- and Mg^{2+} ions in the LCP phase would indicate an electrical behavior resembling that of a "conductor". Further, the decrease in the charge transfer resistance (R_1) may be due to the formation/change of phase and/or films during the cell operation and could be responsible for the electrochemical performance during cycling. The most important difference between Ca- and Mg-ions lies in the nature of formed phase/film which can explain the dramatic difference in the electrochemical performance. The straight successions of circles (LCP), of squares (LCMP) and of triangles (LCCP) in the low frequency range are attributed to the diffusion of the lithium ions into the bulk of the electrode material or so called Warburg diffusion. In the LCP phase, the straight succession of squares (Fig. 5) shows a changing slope to the real axis compared to the LCMP and LCCP phases. This indicates that, close to the $LiCoPO_4$ phase, secondary phases which behave like "resistors" are present in the composites. These phases favor the electron flow in the system but with the irreversible degradation of the electrolyte lead to the formation of side reactions which inhibit the kinetic of the deintercalation/intercalation processes of the Li-ions.

4. Conclusions

In this work the structural, morphological and electrochemical properties of the $LiCo_{0.9}\boldsymbol{M}_{0.1}PO_4$ systems (where $\boldsymbol{M}$ = Co, Mg and Ca) have been investigated.

The X-ray diffraction patterns of the prepared $LiCo_{0.9}M_{0.1}PO_4$ (M = Co, Mg, Ca) powders confirmed the presence of $LiCoPO_4$ with an olivine-like structure as major crystalline phase and revealed a shift in the positions of the (311) and (121) reflections toward higher diffraction angles in the Mg-containing samples and toward lower diffraction angles in the Ca-containing compounds respectively. The shifts can indicate the formation of solid solutions in which the Mg^{2+} and Ca^{2+} ions were successfully introduced into $LiCoPO_4$ matrix structure. The structural analysis showed also the formation of secondary crystalline phases like $Co_2P_2O_7$ and Co_2P and, in the Ca-containing system, Li_3PO_4 and $(Ca,Co)_3(PO_4)_2$ with a non-stoichiometric Ca/Co ratio as further additional phases.

The morphological investigation revealed a spongy-like structured phase on which very small particles of secondary phase(s) can be observed in the $LiCo_{0.9}Co_{0.1}PO_4$ system. A similar structure has been observed in the $LiCo_{0.9}Mg_{0.1}PO_4$ system where the additional growth of almost spherical particles was detected on the surface of the cathode material. The results confirmed the reduction of the Co-containing olivine phosphates leading to the formation of crystallites of Co_2P. In the $LiCo_{0.9}Ca_{0.1}PO_4$ system, more secondary phases including ribbon-like structures have been observed. The latter could correspond to (Co,Ca)-containing phosphates thermodynamically stable at temperatures above 700 °C under nitrogen.

The CV-curves of the LCP phase showed a shoulder at ~4.92 V in anodic sweep and during reverse sweep a cathodic peak at ~4.40 V. The reduction potential of Co^{3+}/Co^{2+} is lower than the value (~4.60–4.65 V) reported in the literature and may be explained by the higher cut-off potential reached during the anodic sweep in this work (5.3 V) where side reactions cannot be ruled out. The CV-curves

of the Mg-containing $LiCoPO_4$ showed a decrease of the voltammetric surface as a function of the anodic and cathodic sweeps and a shift toward higher values of the reduction mean maxima (from 4.52 till 4.63 V). The decrease of cathodic and anodic surface is possibly related to the amount of lithium that can be extracted due to lack of electrochemical activity of the Mg^{2+} ions. On the other hand, the Mg^{2+} ions appear to stabilize the redox active $Co^{2+/3+}$ couple through the Co^{2+}–O–Mg^{2+} interactions leading to a shift of the reduction mean peaks to higher values of potentials. In the CV-curves of the Ca-containing $LiCoPO_4$ phase, important electrochemical events have been observed at 4.80 V and 4.94 V which correspond to the formation the delithiated phases in agreement with the 2-steps delithiation mechanism and at 4.87 V which is a maximum mean peak in the anodic sweep.

The specific capacity as a function of the cycles and the charge and discharge measurements confirm and support the voltammetric data. The specific capacity of the LCP phase at the first cycle (60 mAh g^{-1}) increases compared to the values previously reported by our work; the addition of Mg-ions decreases the specific capacity of the first discharge cycle down to 36 mAh g^{-1} and increases the capacity fade whereas the addition of Ca-ions increases the specific capacity of the first discharge cycle dramatically to 68 mAh g^{-1}. The increase of the specific capacity in the Ca-containing LCP phase can be explained by the decrease of the carbon content and consequently by the lower amount of the Co_2P phase, by their electrochemical activity and by high chemical affinity with the phosphate anions. Furthermore important electrochemical events have been observed at 4.83 V and at 4.90 V respectively confirming the coexistence of a “lithiated” and (partially or totally) “delithiated” phases. We can reasonably assume that at values higher than 4.90 V the LCCP phase is (totally) delithiated. Indeed, the Ca-ions seem to favor the stabilization of the “$CoPO_4$ amorphous phase”, possibly either due to a rearrangement of the charge distribution of the non-bridge oxygen atoms (O···Ca^{2+} ···O) or by avoid the release of the oxygen during the discharge process.

The impedance measurements performed before cycling support the previous data, showing a decrease of the charge transfer resistance from 104 Ω for the LCP phase to 81 Ω and 62 Ω for the Mg- and Ca-containing LCP phase respectively and an improvement of the Li-ions diffusion. The decrease in the charge transfer resistance may be due to the formation/change of phase and/or films during the cell operation and could be responsible for the electrochemical performance during cycling. The most important difference between Ca- and Mg-ions lies in the nature of formed phase/film which can explain the dramatic difference in the electrochemical performance.

Acknowledgments

Many thanks are owed to Mr. J.-C. Jaud for the technical assistance in the XRD analysis.

The authors thank the *Deutsche Forschungsgemeinschaft* (DFG) (*Sonderinitiativeproject: PAK-177*) for the financial support during this work. The DFG encourage and financially support the publication of the results during the projects. The DFG have no involvement in study design; in analysis and interpretation of data; in the writing of the report; and in the decision to submit the paper for publication.

Appendix A. Supplementary data

Supplementary data related to this article can be found at http://dx.doi.org/10.1016/j.jpowsour.2013.05.196.

References

[1] D.W. Han, Y.M. Kang, R.Z. Yin, M.S. Song, H.S. Kwon, Electrochem. Commun. 11 (2009) 137–140.
[2] A.K. Padhi, K.S. Nanjundaswami, J.B. Goodenough, J. Electrochem. Soc. 144 (1997) 1188–1194.
[3] G. Li, H. Azuma, M. Tohda, Electrochem Solid-State Lett. 5 (2002) A135–A137.
[4] C. Delacourt, L. Laffont, R. Bouchet, C. Wurm, J.-B. Leriche, M. Morcrette, J.-M. Tarascon, C. Masquelier, J. Electrochem. Soc. 152 (2005) A913–A921.
[5] K. Amine, H. Yasuda, Y. Yamachi, Electrochem. Solid-State Lett. 3 (2000) 178–179.
[6] N.N. Bramnik, K. Nikolowski, C. Baehtz, K.G. Bramnik, H. Ehrenberg, Chem. Mater. 19 (2007) 908–915.
[7] J. Wolfenstine, J. Allen, J. Power Sources 136 (2004) 150–153.
[8] S. Okada, S. Sawa, M. Egashira, J. Yamaki, M. Tabuchi, H. Kageyama, T. Konishi, A. Yoshino, J. Power Sources 97–98 (2001) 430–432.
[9] M. Nakayama, S. Goto, Y. Uchimoto, M. Wakihara, Y. Kitajima, Chem. Mater. 16 (2004) 3399–3401.
[10] J.M. Lloris, C. Pérez Vicente, J.L. Tirado, Electrochem. Solid-State Lett. 5 (2002) A234–A237.
[11] B. Jin, H.B. Gu, K.W. Kim, J. Solid-State Electrochem. 12 (2008) 105–111.
[12] A. Nytén, J.O. Thomas, Solid State Ionics 177 (2006) 1327–1330.
[13] M.S. Islam, D.J. Driscoll, C.A.J. Fisher, P.R. Slater, Chem. Mater. 17 (2005) 5085–5092.
[14] C.A.J. Fisher, V.M. Hart Prieto, M.S. Islam, Chem. Mater. 20 (2008) 5907–5915.
[15] N.N. Bramnik, K. Nikolowski, D.M. Trots, H. Ehrenberg, Electrochem. Solid-State Lett. 11 (2008) A89–A93.
[16] Gangulibabu, D. Bhuvaneswari, N. Kalaiselvi, N. Jayaprakash, P. Periasamy, J. Sol-Gel Sci. Technol. 49 (2009) 137–144.
[17] M.S. Bhuwaneswari, L. Dimesso, W. Jaegermann, J. Sol-Gel Sci. Technol. 56 (2010) 320–326.
[18] R. Vasanthi, D. Kalpana, N.G. Renganathan, J. Solid-State Electrochem. 12 (2008) 961–969.
[19] L. Dimesso, S. Jacke, C. Spanheimer, W. Jaegermann, J. Solid State Electrochem. 16 (2012) 911–919.
[20] L. Dimesso, S. Cherkashinin, C. Spanheimer, W. Jaegermann, J. Alloys Compd. 516 (2012) 119–125.
[21] M. Schmidt, U. Heider, K. Kuehner, R. Oesten, M. Jungnitz, N. Ignatev, P. Sartor, J. Power Sources 97–98 (2001) 557–560.
[22] J.S. Gnanaraj, E. Zinigrad, M.D. Levi, D. Aurbach, M. Schmidt, J. Power Sources 119–121 (2003) 799–804.
[23] T. Muraliganth, A. Manthiram, J. Phys. Chem. C 114 (2010) 15530–15540.
[24] M.V.V.M. Satya Kishore, U.V. Varadaraju, Mater. Res. Bull. 40 (2005) 1705–1712.
[25] R.D. Shannon, Acta Cryst. A32 (1976) 751–767.
[26] P.S. Herle, B. Ellis, N. Coombs, L.F. Nazar, Nat. Mater. 3 (2004) 147–152.
[27] S. Raynaud, E. Champion, D. Bernache-Assollant, Biomaterials 23 (2002) 1073–1080.
[28] J. Xie, N. Imanishi, T. Zhang, A. Hirano, Y. Takeda, O. Yamamoto, J. Power Sources 192 (2009) 689–692.
[29] L. Tan, Z. Luo, H. Liu, Y. Yu, J. Alloys Compd. 502 (2010) 407–410.
[30] Y.H. Rho, L.F. Nazar, L. Perry, D. Ryan, J. Electrochem. Soc. 154 (2007) A283–A289.
[31] M. Hayashi, H. Arai, H. Ohtsuka, Y. Sakurai, J. Power Sources 119–121 (2003) 617–620.
[32] J. Wolfenstine, J. Read, J.L. Allen, J. Power Sources 163 (2007) 1070–1073.
[33] H. Huang, S.-C. Yin, L.F. Nazar, Electrochem. Solid-State Lett. 4 (2001) A170–A172.
[34] F. Hanic, M. Handlovic, K. Burdova, J. Majling, J. Chrystallogr, Spectrosc. Res. 12 (1982) 99–127.
[35] Y. Sakurai, S. Okada, J. Yamaki, T. Okada, J. Power Sources 20 (1987) 173–177.
[36] J.L. Allen, T.R. Jow, J. Wolfenstine, J. Power Sources 196 (2011) 8656–8661.
[37] P. Lightfoot, M.C. Pienkowski, P.G. Bruce, I. Abrahams, J. Mater. Chem. 1 (1991) 1061–1063.
[38] B. Louati, K. Guidara, Ionics 17 (2011) 633–640.
[39] J. Ni, L. Gao, L. Lu, J. Power Sources 221 (2013) 35–41.
[40] L. Dimesso, C. Spanheimer, W. Jagermann, Y. Zhang, A.L. Yarin, Electrochim. Acta 95 (2013) 38–42.
[41] L. Dimesso, D. Becker, C. Spanheimer, W. Jaegermann, J. Sol. State Electrochem. 16 (2012) 3791–3798.